「なぜ宇宙は加速するのか? - 徹底的究明と将来への挑戦 -」
発足シンポジウム
20-21 September 2015, Kavli IPMU

The Origin of Cosmic Objects

Masayuki Umemura

Center for Computational Sciences
University of Tsukuba

3D Problems in Cosmology

Dark Matter: How was dark matter generated?

Dark Energy: What accelerates the Universe?

Dark Age: What is the origin of cosmic objects?

→ FIRST^3: First Stars, First Galaxies, First BHs

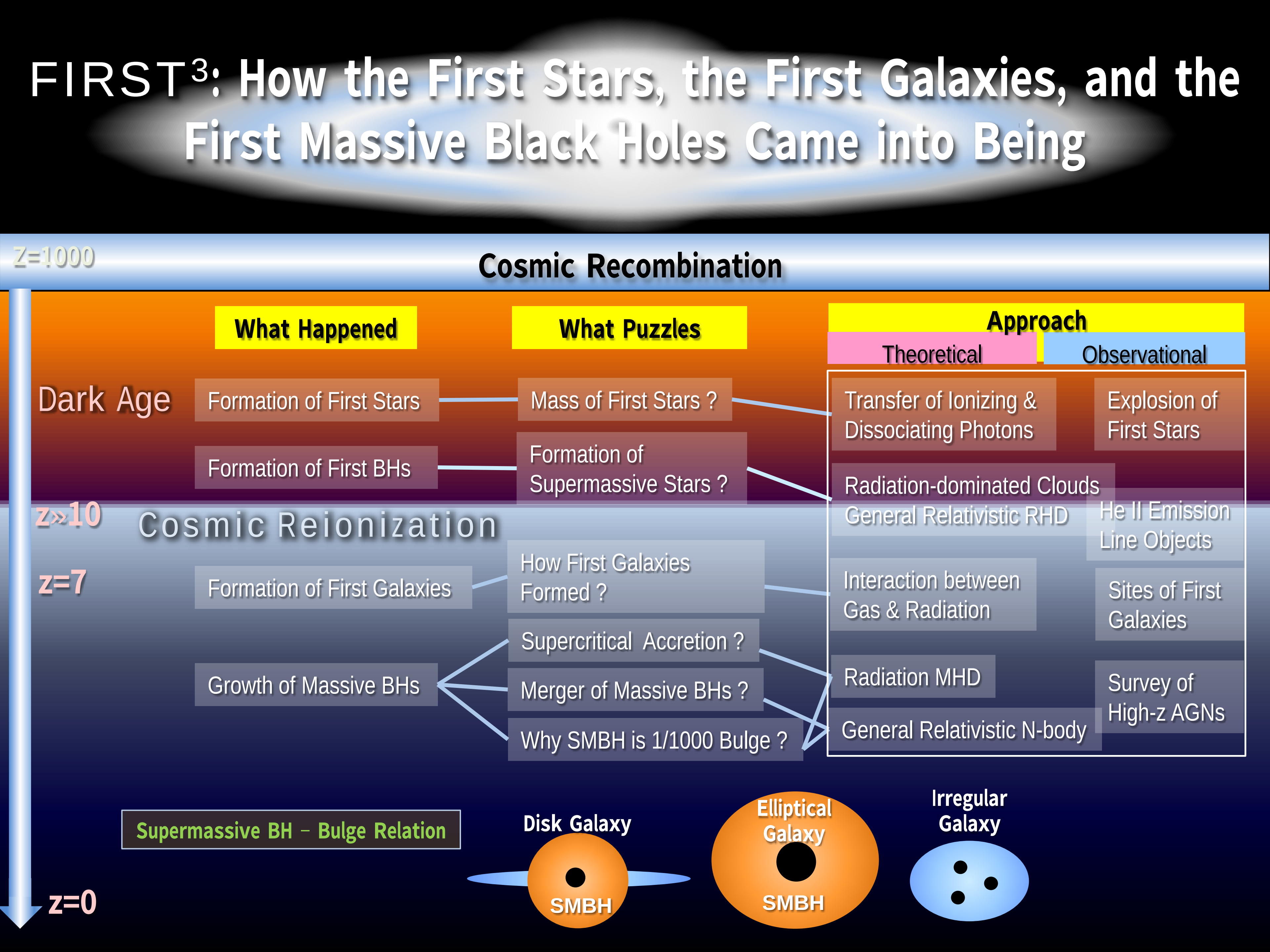
FIRST³: How the First Stars, the First Galaxies, and the First Massive Black Holes Came into Being
Z=1000
Cosmic Recombination
What Happened
What Puzzles
Approach
Theoretical
Observational
Dark Age
Formation of First Stars
Mass of First Stars ?
Transfer of Ionizing & Dissociating Photons
Explosion of First Stars
Formation of First BHs
Formation of Supermassive Stars ?
Radiation-dominated Clouds General Relativistic RHD
He II Emission Line Objects
z»10
Cosmic Reionization
z=7
Formation of First Galaxies
How First Galaxies Formed ?
Interaction between Gas & Radiation
Sites of First Galaxies
Supercritical Accretion ?
Growth of Massive BHs
Merger of Massive BHs ?
Radiation MHD
Survey of High-z AGNs
Why SMBH is 1/1000 Bulge ?
General Relativistic N-body
Supermassive BH – Bulge Relation
Disk Galaxy
SMBH
Elliptical Galaxy
SMBH
Irregular Galaxy
z=0

Supermassive BH-Bulge Relation

Kormendy & Richstone 1995
Magorrian et al. 1998
Marconi & Hunt 2003
Kormendy & Ho 2013

M_{BH} / M_{bulge} » 0.001

Kormendy & Ho 2013, ARA&A, 51, 511

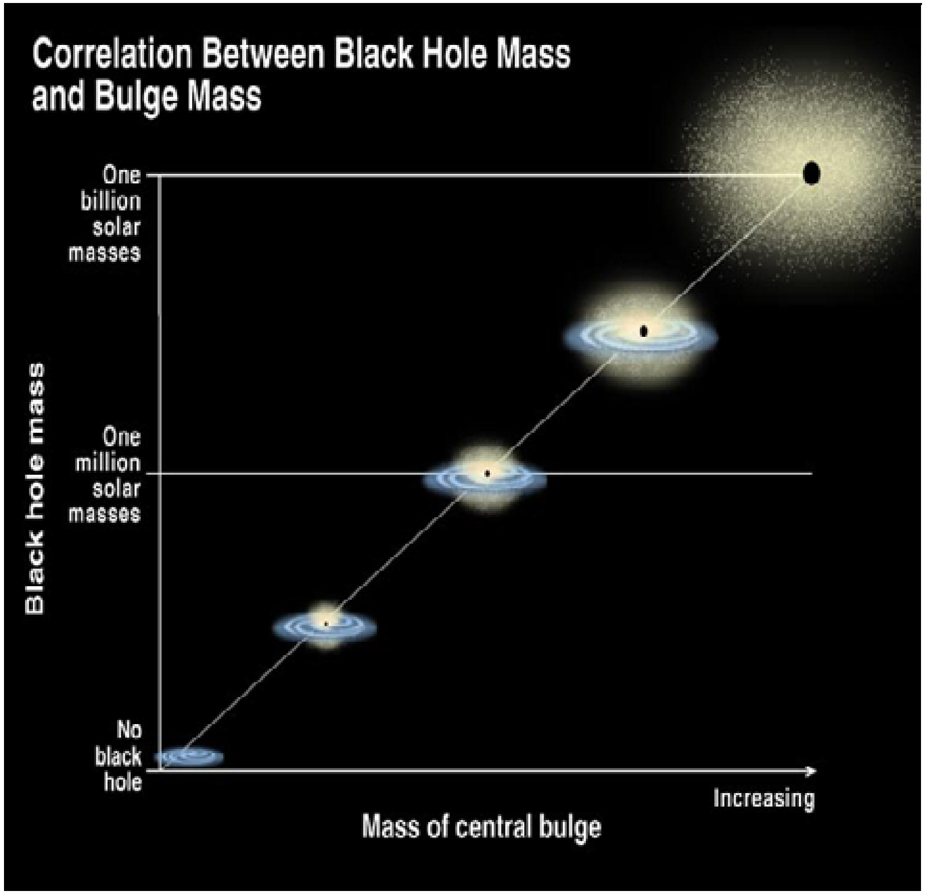

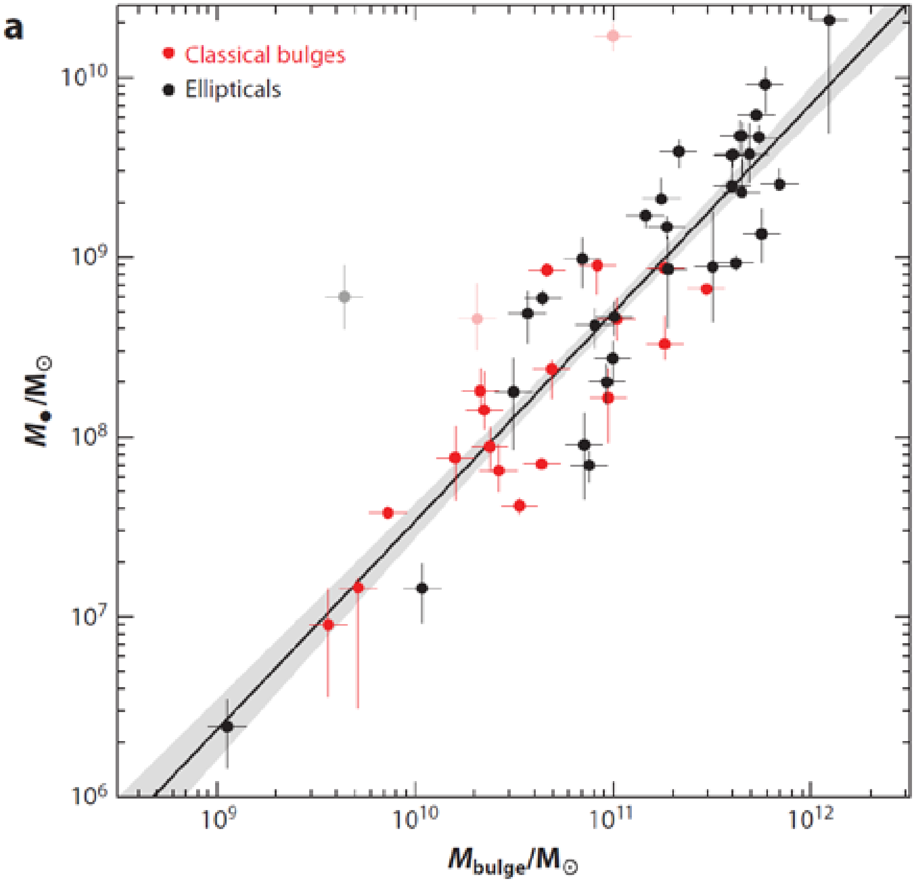

z=7.085 QSO (0.8Gyr)

Mortlock et al. 2011, nature, 474, 616

L=6.3´ $10^{13}L_{¤}$, M_{BH}=2´ $10^{9}M_{¤}$

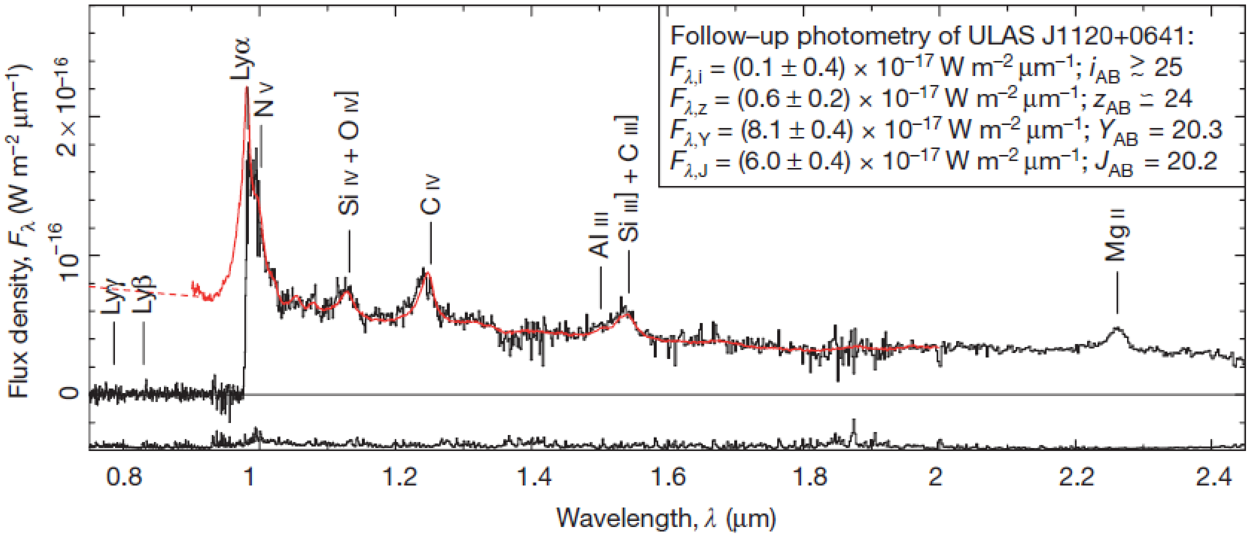

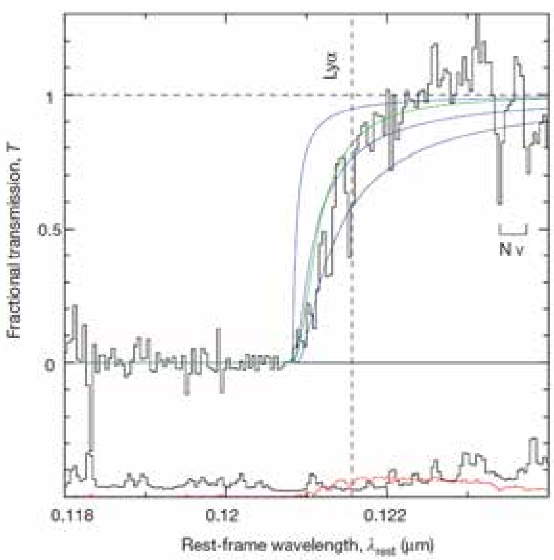

Figure 4 | Rest-frame transmission profile of ULAS J1120+0641 in the region of the Lyα emission line, compared to several damping profiles. The transmission profile of ULAS J1120+0641, obtained by dividing the spectrum by the SDSS composite shown in Fig. 1, is shown in black. The random error spectrum is plotted below the data, also in black. The positive residuals near 0.1230 μm in the transmission profile suggest that the Lyα emission line of ULAS J1120+0641 is actually stronger than average, in which case the absorption would be greater than illustrated. The dispersion in the Lyα equivalent width at a fixed C IV equivalent width of 13% quantifies the uncertainty in the Lyα strength; this systematic uncertainty in the transmission profile is shown in red. The blue curves show the Lyα damping wing of the intergalactic medium for neutral fractions of (from top to bottom) $f_{HI} = 0.1$, $f_{HI} = 0.5$ and $f_{HI} = 1.0$, assuming a sharp ionization front 2.2 Mpc in front of the quasar. The green curve shows the absorption profile of a damped Lyα absorber of column density $N_{HI} = 4 \times 10^{20}$ cm^{-2} located 2.6 Mpc in front of the quasar. These curves assume that the ionized zone itself is completely transparent; a more realistic model of the H I distribution around the quasar might be sufficient to discriminate between these two models[25-27]. The wavelength of the Lyα transition is shown as a dashed line; also marked is the N V doublet of the associated absorber referred to in the text.

z=6.30 QSO (0.9Gyr)

Xue-BingWu et al. 2015, nature, 518, 512

L=4.29´ $10^{14}L$¤ , M_{BH}=1.2´ $10^{10}M$¤

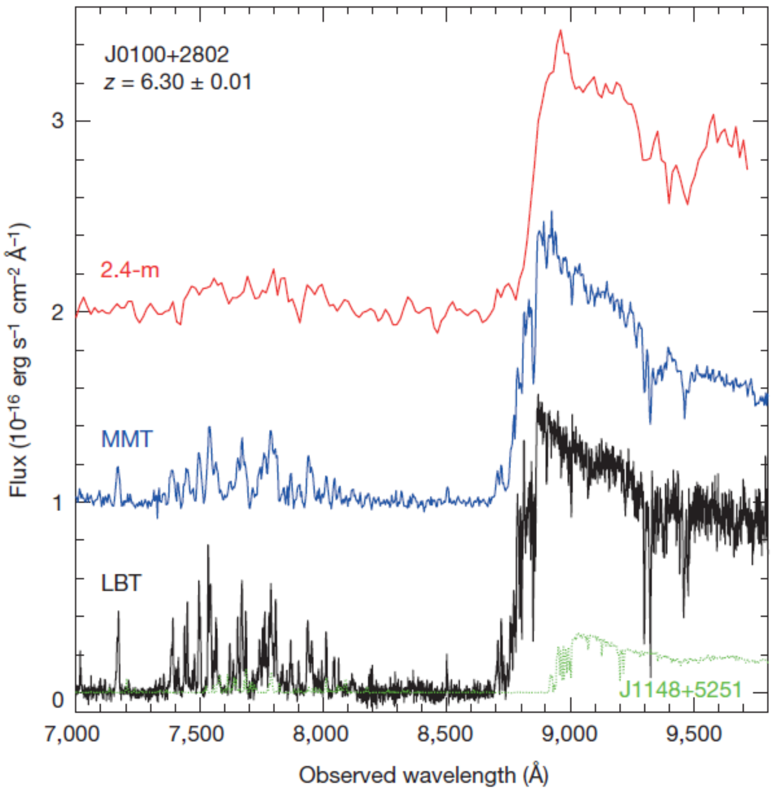

Figure 1 | The optical spectra of J0100+2802. From top to bottom, spectra taken with the Lijiang 2.4-m telescope, the MMT and the LBT (in red, blue and black colours), respectively. For clarity, two spectra are offset upward by one and two vertical units. Although the spectral resolution varies from very low to medium, in all spectra the Lyα emission line, with a rest-frame wavelength of 1,216 Å, is redshifted to around 8,900 Å, giving a redshift of 6.30. J0100+2802 is a weak-line quasar with continuum luminosity about four times higher than that of SDSS J1148+5251 (in green on the same flux scale)[1], which was previously the most luminous high-redshift quasar known at $z = 6.42$.

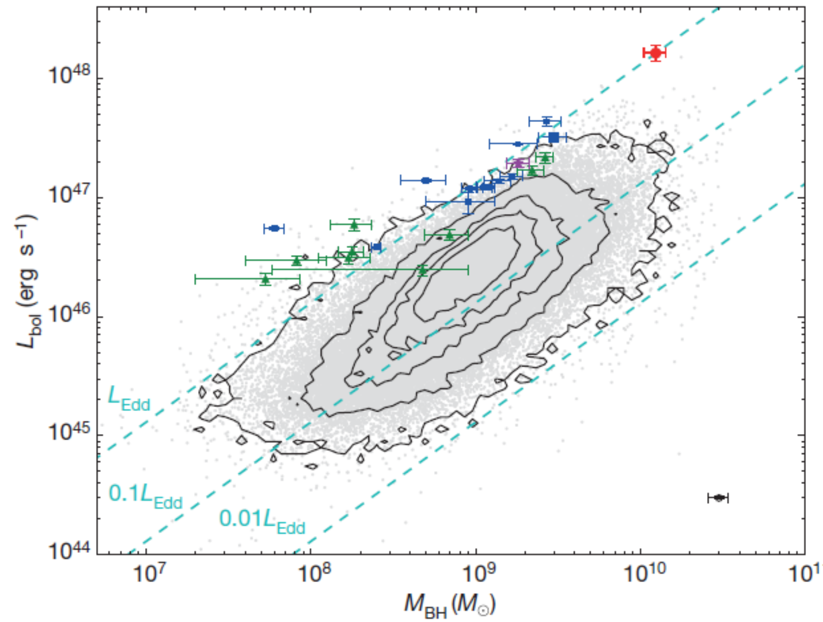

Figure 4 | Distribution of quasar bolometric luminosities, L_{bol}, and black-hole masses, M_{BH}, estimated from the Mg II lines. The red circle at top right represents J0100+2802. The small blue squares denote SDSS high-redshift quasars[2,10,12], and the large blue square represents J1148+5251. The green triangles denote CFHQS high-redshift quasars[11,12]. The purple star denotes ULAS J1120+0641 at $z = 7.085$ (ref. 6). Black contours (which indicate 1σ to 5σ significance from inner to outer) and grey dots denote SDSS low-redshift quasars[21] (with broad absorption line quasars excluded). Error bars represent the 1σ standard deviation, and the mean error bar for low-redshift quasars is presented in the bottom-right corner. The dashed lines denote the luminosity in different fractions of the Eddington luminosity, L_{Edd}. Note that the black-hole mass and bolometric luminosity are calculated using the same method and the same cosmology model as in the present Letter, and the systematic uncertainties (not included in the error bars) of virial black-hole masses could be up to a factor of three[27].

Mass Accretion onto BH

Machida et al. 2004

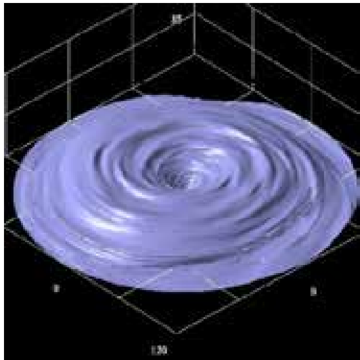

1pc ® BH

Ohsuga et al. 2005

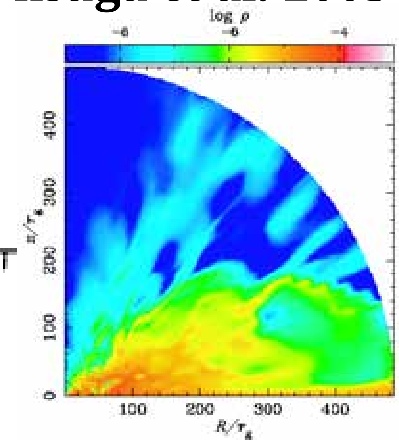

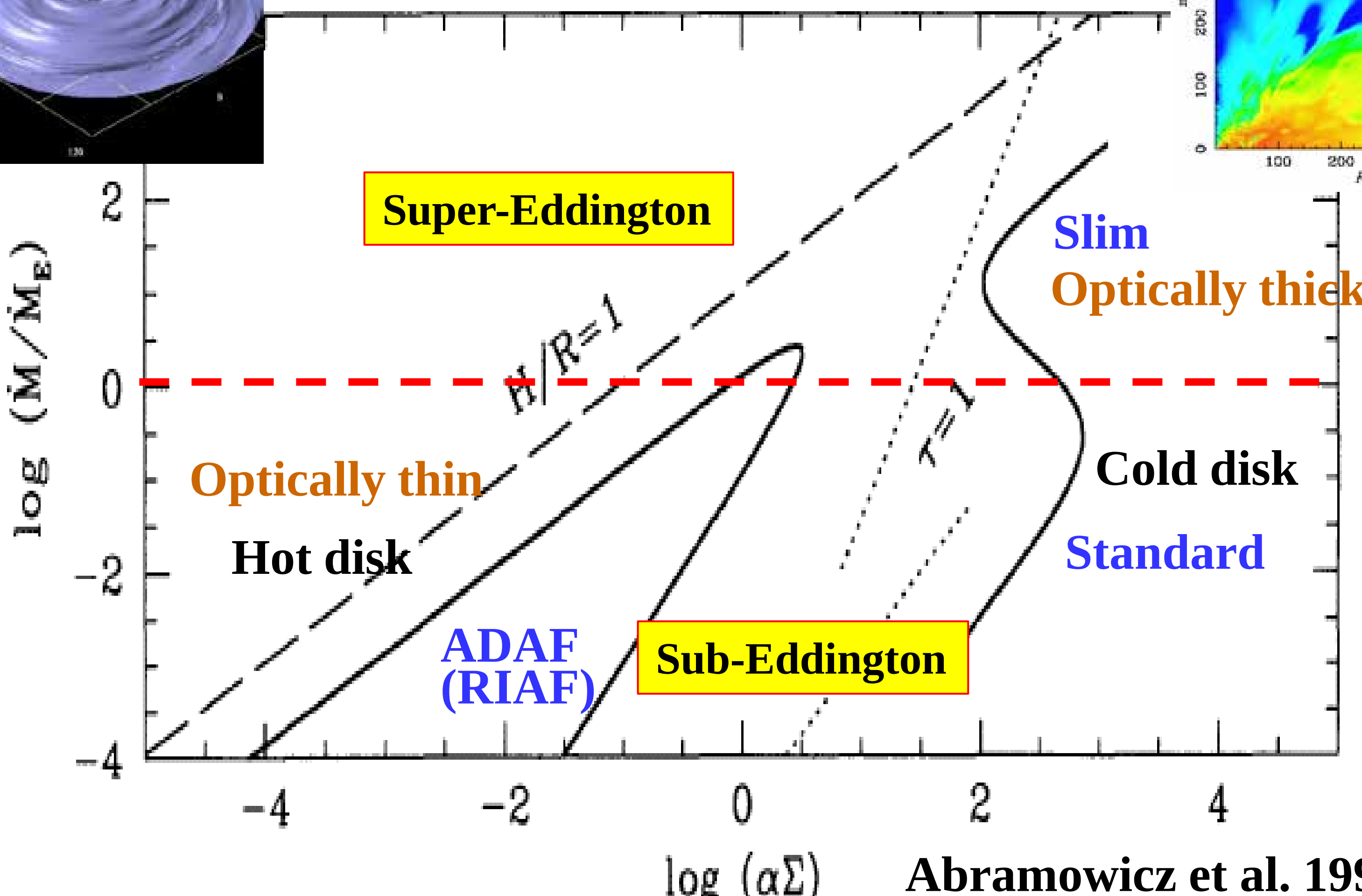

Abramowicz et al. 1995

Energy Conversion Efficiency in Accretion Flows

$$L = \eta \dot{M} c^2, \quad L_E = \frac{4\pi G c m_p M_{BH}}{\sigma_T} = \eta \dot{M}_E c^2$$

$$t_E \equiv \frac{M}{\dot{M}_E} = 4.5 \times 10^7 \left(\frac{\eta}{0.1}\right) \mathrm{yr}$$

① Sub-Eddington: RIAF (Radiatively Inefficient Accretion Flow)

Eddington ratio $\quad \nu_E \equiv \frac{\dot{M}}{\dot{M}_E} = 1 \;\Rightarrow\; \eta \approx 0.1 \frac{\dot{M}}{\dot{M}_E}$

② Eddington: Standard Disk

$$\nu_E \equiv \frac{\dot{M}}{\dot{M}_E} \approx 1 \;\Rightarrow\; \eta \approx 0.1$$

③ Super-Eddington: Slim Disk (Photon trapping)

$$\nu_E \equiv \frac{\dot{M}}{\dot{M}_E} > 1 \;\Rightarrow\; \eta \approx 0.1 \left(\frac{\dot{M}}{\dot{M}_E}\right)^{-1/2}$$

Eddington Growth of z=7.085 QSO SMBH

$$M_{BH}(t) = M_0 \exp\left(\nu_E \frac{t}{t_E}\right), \quad t_E \equiv \frac{M}{\dot{M}_E} = 4.5 \times 10^7 \left(\frac{\eta}{0.1}\right) \mathrm{yr}$$

$$z_{PopIII} = 20 \; (t = 1.83 \times 10^8 \mathrm{yr}), \;\; M_0 = 20 M_\odot$$

$$z_{QSO} = 7.085 \; (t = 7.83 \times 10^8 \mathrm{yr}), \;\; M_{BH} = 2 \times 10^9 M_\odot$$

$$\Delta t = 6 \times 10^8 \mathrm{yr}$$

$$\nu_E = 1.4$$ **Super-Eddington**

Eddington Growth of z=6.30 QSO SMBH

$$M_{BH}(t) = M_0 \exp\left(\nu_E \frac{t}{t_E}\right), \quad t_E \equiv \frac{M}{\dot{M}_E} = 4.5 \times 10^7 \left(\frac{\eta}{0.1}\right) \mathrm{yr}$$

$$z_{PopIII} = 20 \ (t = 1.83 \times 10^8 \mathrm{yr}), \ M_0 = 20 M_\odot$$

$$z_{QSO} = 6.30 \ (t = 8.84 \times 10^8 \mathrm{yr}), \ M_{BH} = 1.2 \times 10^{10} M_\odot$$

$$\Delta t = 7.01 \times 10^8 \mathrm{yr}$$

$$\nu_E = 1.3$$ **Super-Eddington**

But, the mass accretion should be intermittent. (Milosavljevic+2009a,b)

When & How First Massive Black Holes Came into being

Rees Diagram
(1984)

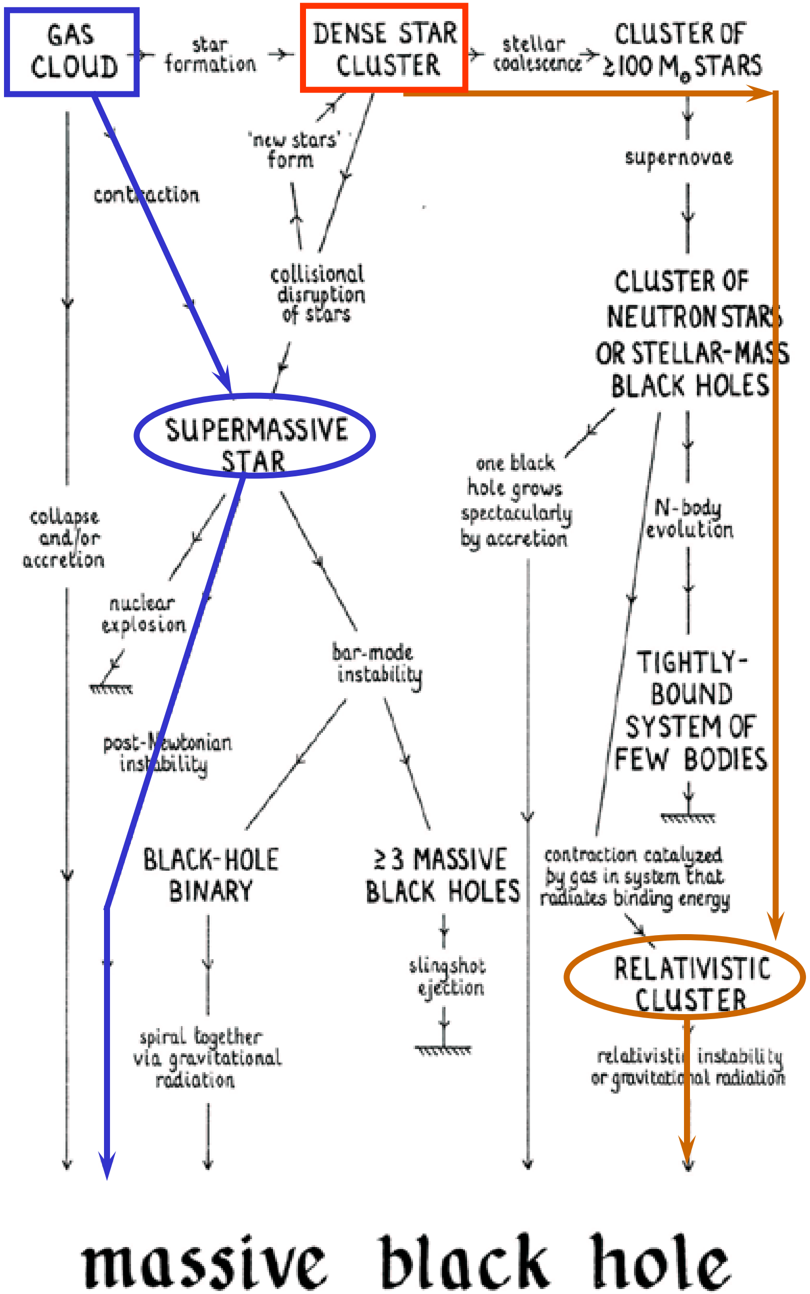

Figure 1 Schematic diagram [reproduced from Rees (106)] showing possible routes for runaway evolution in active galactic nuclei.

Cosmological Rees Diagram

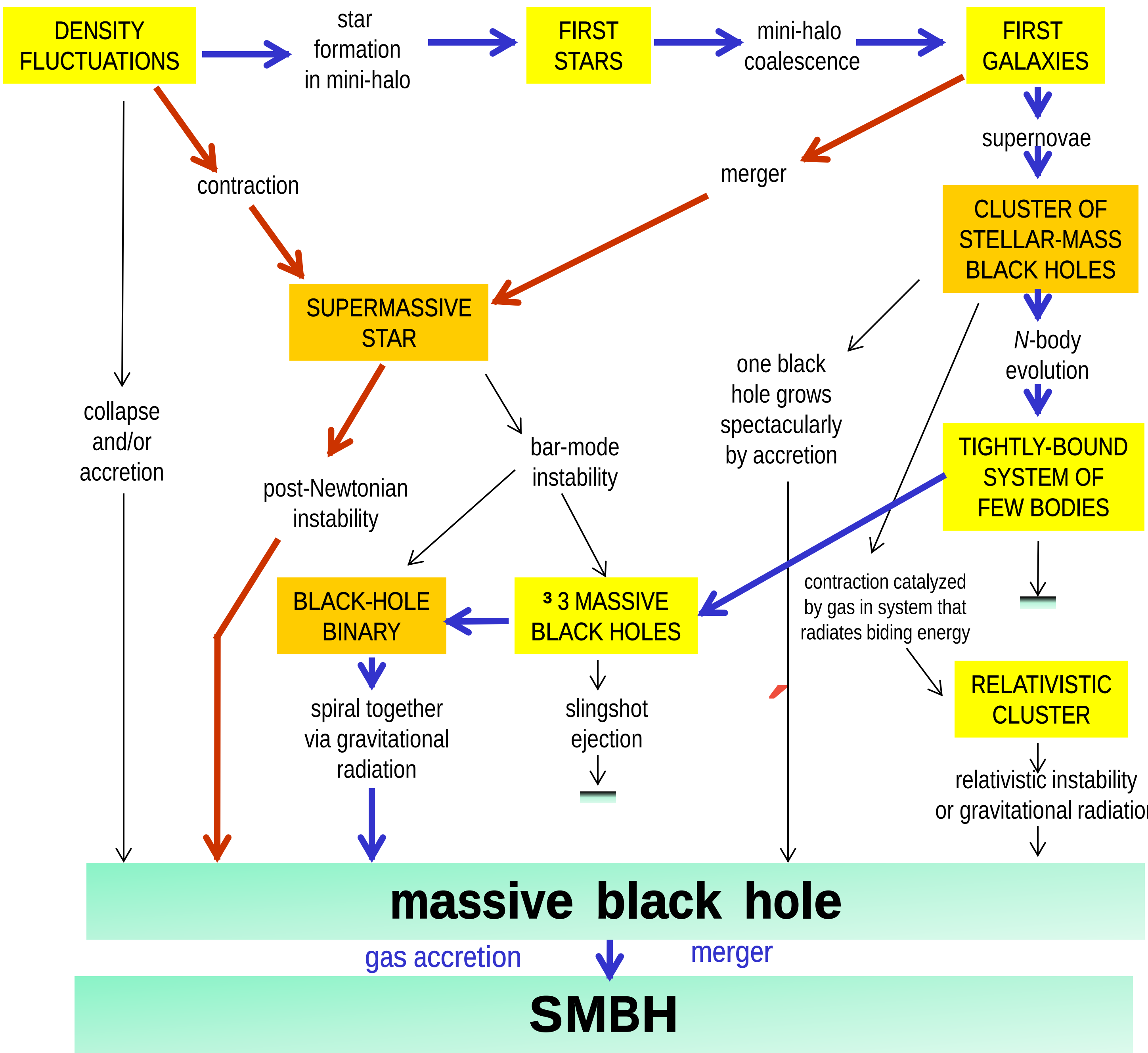

Mass of First Stars

- a few $100M_{\odot}$ (Abel et al. 2000; Bromm et al. 2002; Yoshida et al. 2006)
- $\sim M_{\odot}$ or a few $100M_{\odot}$ (Nakamura & Umemura 2001)
- several $10M_{\odot}$ (Clark et al. 2011)
- about $40M_{\odot}$ (Hosokawa et al. 2011)
- a few – $10M_{\odot}$ (Greif et al. 2011)

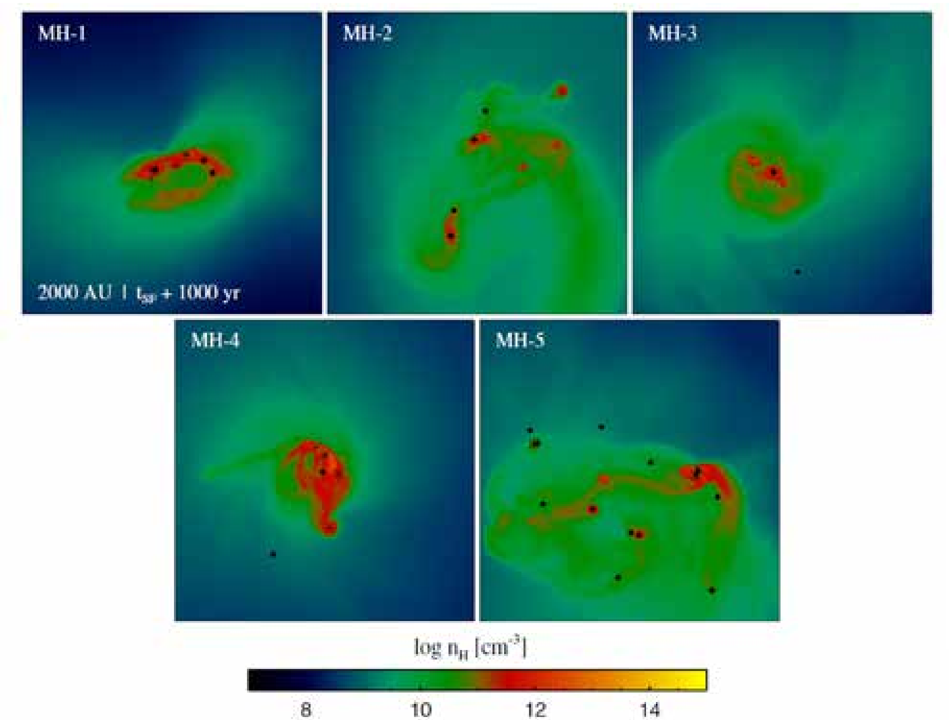

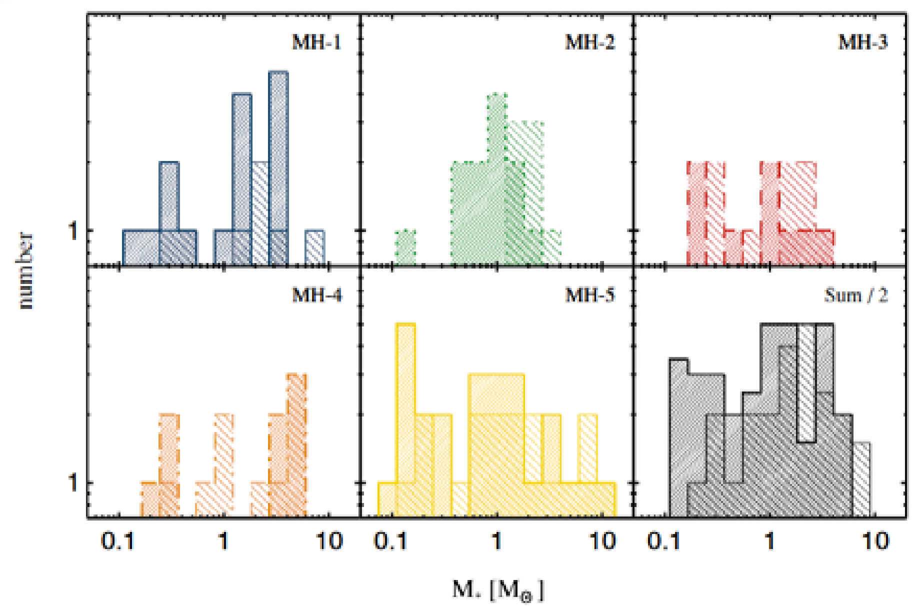

Mass of First Stars: Revisited

Susa, Hasegawa, Tominaga, 2014, ApJ, 792, 32

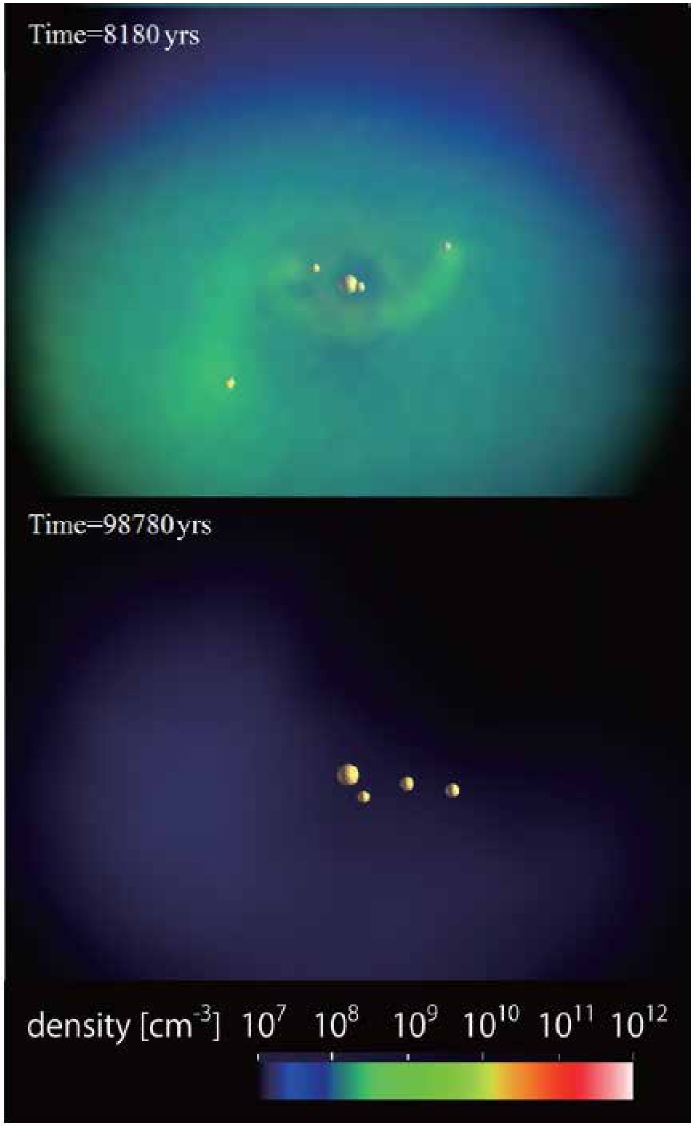

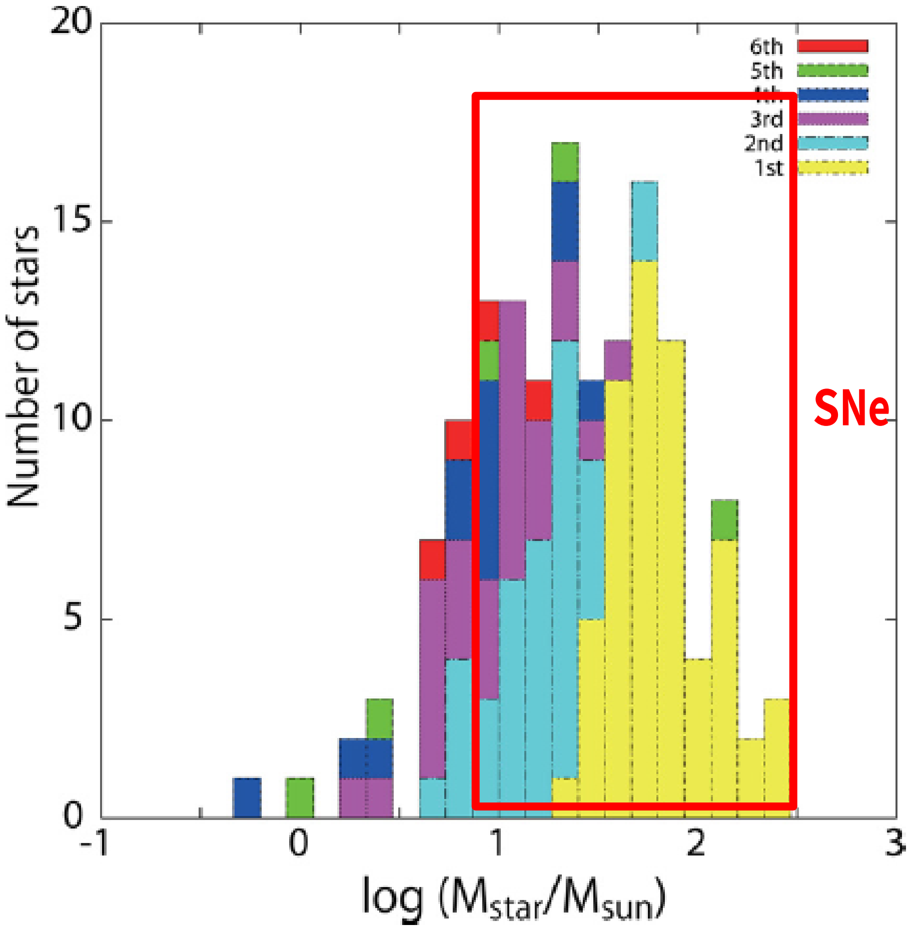

Figure 9. Mass spectrum of first stars is shown. The colors in the histogram correspond to the order of birth of these stars. The color legend in the upper right corner describes the correspondence between the order of birth and the color.

Pop III Star Evolution

Heger & Woosley 2002, ApJ, 567, 532

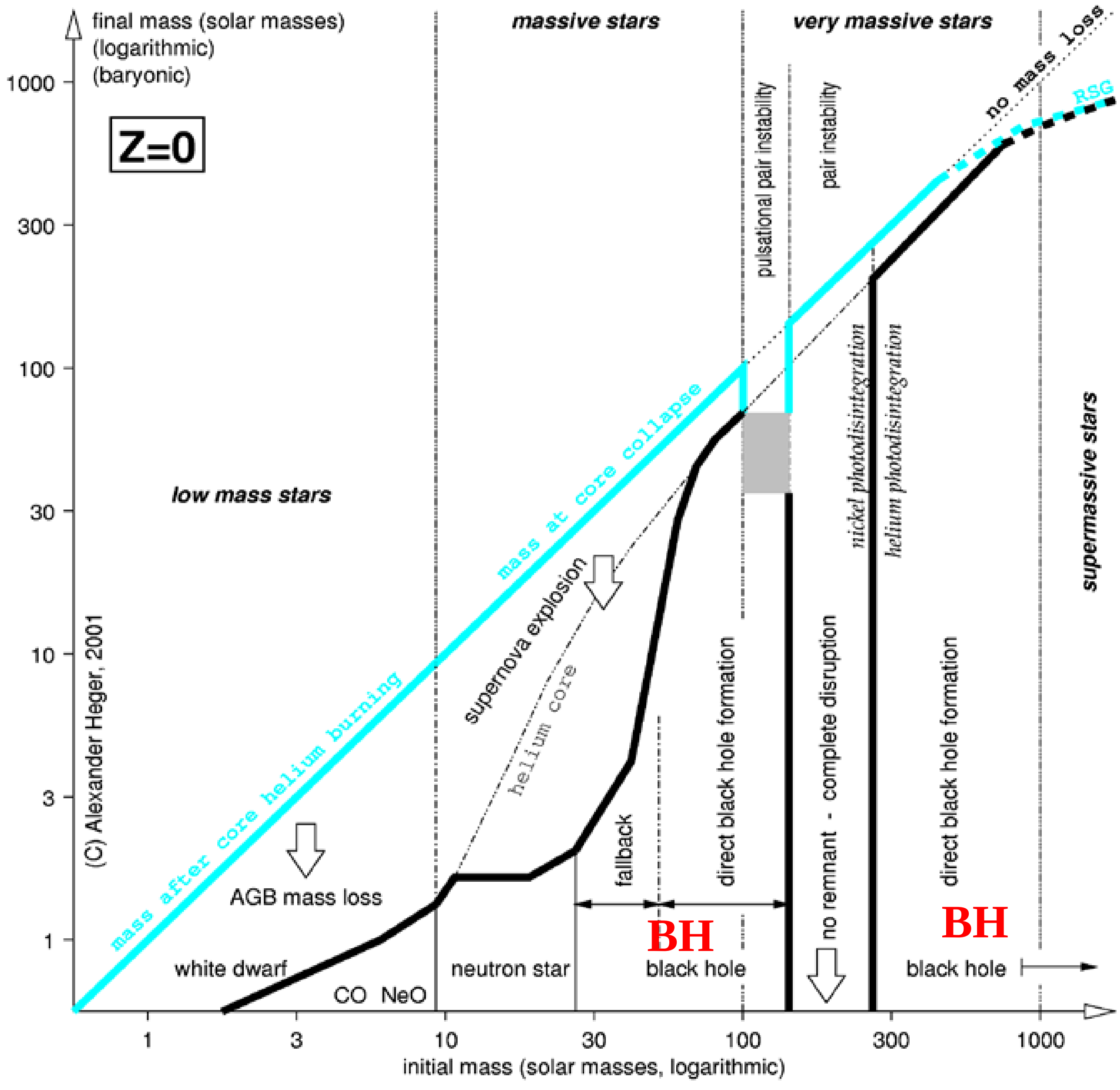

Early Cosmic Merger of Multiple Black Holes

Tagawa, Umemura, Gouda, Yano & Yamai, 2015, MNRAS, 451, 2174

BH merger via gas dynamical friction with general relativistic effects

$$\mathrm{a}_{\mathrm{DF},i}^{\mathrm{gas}} = -4\pi G^2 m_i m_{\mathrm{H}} n_{\mathrm{gas}}(r) \frac{\mathbf{v}_i}{{v_i}^3} \times f(\mathcal{M}_i)$$

$$f(\mathcal{M}_i) = \begin{cases} 0.5\ln\left(\frac{v_i t}{r_{\min}}\right)\left[\mathrm{erf}\left(\frac{\mathcal{M}_i}{\sqrt{2}}\right) - \sqrt{\frac{2}{\pi}}\mathcal{M}_i \exp(-\frac{\mathcal{M}_i^2}{2})\right] \\ (0 \leqslant \mathcal{M}_i \leqslant 0.8) \\ 1.5\ln\left(\frac{v_i t}{r_{\min}}\right)\left[\mathrm{erf}\left(\frac{\mathcal{M}_i}{\sqrt{2}}\right) - \sqrt{\frac{2}{\pi}}\mathcal{M}_i \exp(-\frac{\mathcal{M}_i^2}{2})\right] \\ (0.8 \leqslant \mathcal{M}_i \leqslant \mathcal{M}_{eq}) \\ \frac{1}{2}\ln\left(1 - \frac{1}{\mathcal{M}_i^2}\right) + \ln\left(\frac{v_i t}{r_{\min}}\right), \\ (\mathcal{M}_{eq} \leqslant \mathcal{M}_i) \end{cases}$$

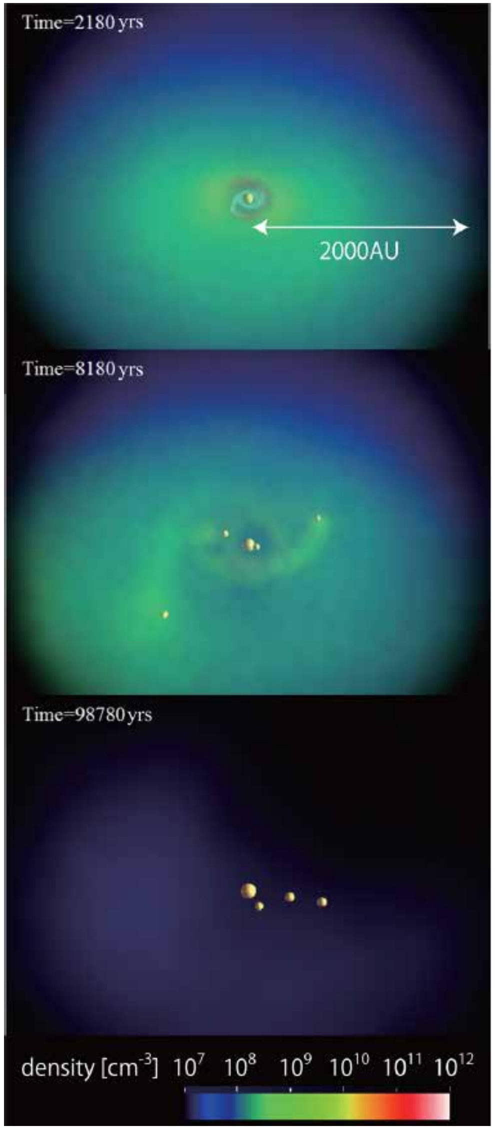

Susa, Hasegawa & Tominaga 2014

The separation of the closest pair

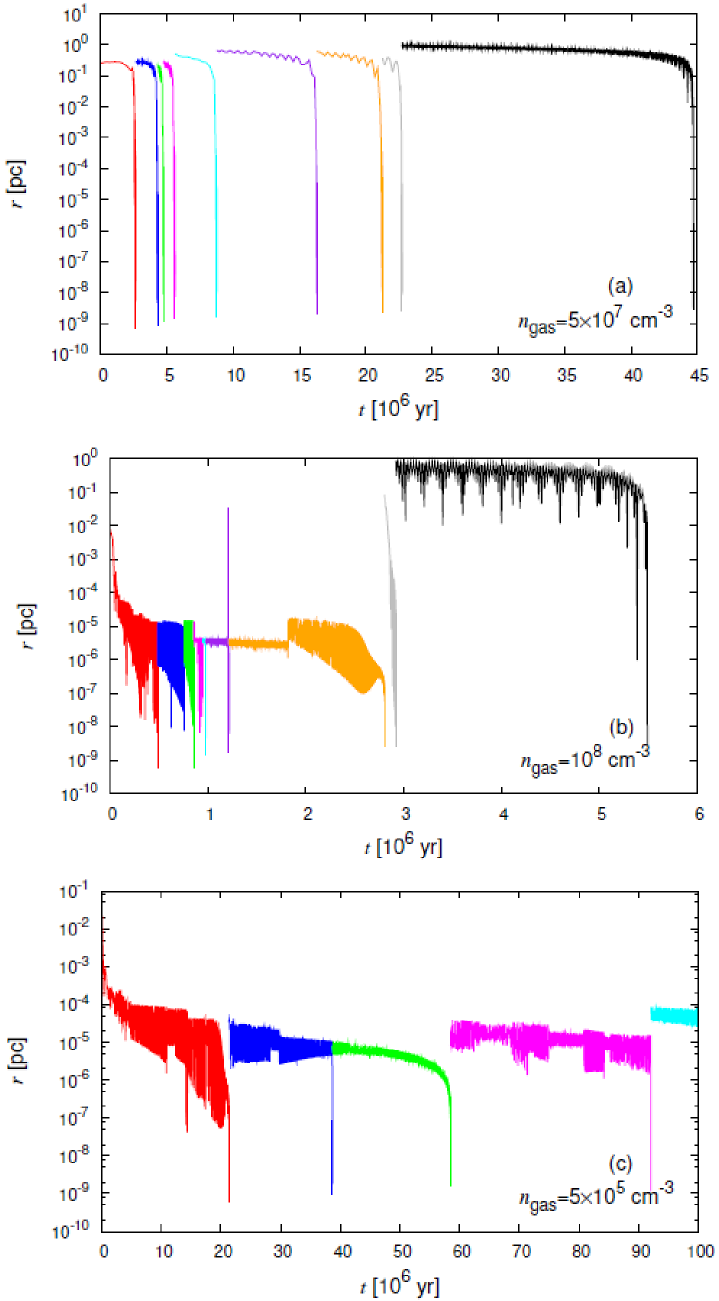

Type A

Gas-drag-driven merger

Type B

Interplay-driven merger
(Three body-driven and thereafter gas-drag-driven merger)

Type C

Three body-driven merger

All BHs in the First Objects can merger into one in 10^7yr !

Table 1. The results with $M_{\rm BH} = 30\ M_\odot$ and $N_{\rm BH} = 10$.

$r_{\rm typ}$[pc]	1.0			0.464			0.215			0.1			0.0464			0.0215			0.01		
$\rho_{\rm BH}[M_\odot {\rm pc}^{-3}]$	7.2×10^1			7.2×10^2			7.2×10^3			7.2×10^4			7.2×10^5			7.2×10^6			7.2×10^7		
$n_{\rm gas}[{\rm cm}^{-3}]$	$N_{\rm m}$	type	$t_{\rm fin}$[yr]	$N_{\rm m}$	type	$t_{\rm fin}$[yr]	$N_{\rm m}$	type	$t_{\rm fin}$[yr]	$N_{\rm m}$	type	$t_{\rm fin}$[yr]	$N_{\rm m}$	type	$t_{\rm fin}$[yr]	$N_{\rm m}$	type	$t_{\rm fin}$[yr]	$N_{\rm m}$	type	$t_{\rm fin}$[yr]
10^{12}	0	-	1.0×10^8	5	A	1.0×10^8	9	A	3.6×10^7	9	A	4.4×10^6	9	A	1.7×10^6	9	A	7.0×10^5	9	B	4.3×10^5
10^{11}	2	A	1.0×10^8	8	A	1.0×10^8	9	A	1.3×10^7	9	A	1.8×10^5	9	A	1.8×10^5	9	A	2.3×10^4	9	B	2.8×10^4
10^{10}	5	A	1.0×10^8	9	A	4.5×10^7	9	A	5.1×10^6	9	A	5.9×10^5	9	A	7.4×10^4	9	B	6.3×10^4	9	B	1.7×10^5
5×10^9	5	A	1.0×10^8	9	A	2.9×10^7	9	A	3.1×10^6	9	A	4.5×10^5	9	B	1.6×10^5	9	B	3.4×10^5	9	B	7.7×10^4
10^9	8	A	1.0×10^8	9	A	2.4×10^7	9	A	3.5×10^6	9	B	2.6×10^5	9	B	4.3×10^5	9	B	3.5×10^5	9	B	3.0×10^5
5×10^8	8	A	1.0×10^8	9	A	1.2×10^7	9	A	1.3×10^6	9	B	6.5×10^5	9	B	4.3×10^5	9	B	5.5×10^5	9	B	5.1×10^5
10^8	9	A	3.0×10^7	9	A	5.1×10^6	9	B	4.0×10^6	9	B	5.5×10^6	9	B	3.6×10^6	9	B	4.2×10^6	9	B	1.2×10^7
5×10^7	9	A	4.5×10^7	9	B	3.7×10^6	9	B	2.2×10^7	9	B	3.2×10^7	9	B	1.3×10^7	9	B	4.7×10^6	9	B	3.6×10^6
10^7	9	B	3.8×10^7	9	B	2.3×10^7	9	B	1.7×10^7	9	B	3.3×10^7	9	B	1.8×10^7	9	B	2.9×10^7	9	B	1.7×10^7
5×10^6	9	B	4.2×10^7	9	B	3.9×10^7	9	B	4.2×10^7	9	B	4.7×10^7	9	B	6.3×10^7	9	B	3.5×10^7	9	B	3.1×10^7
10^6	6	B	1.0×10^8	6	B	1.0×10^8	8	B	1.0×10^8	6	C	1.0×10^8	8	C	1.0×10^8	6	C	1.0×10^8	6	C	1.0×10^8
5×10^5	2	C	1.0×10^8	6	C	1.0×10^8	6	C	1.0×10^8	4	C	1.0×10^8	5	C	1.0×10^8	3	C	1.0×10^8	4	C	1.0×10^8
10^5	0	-	1.0×10^8	0	-	1.0×10^8	1	C	1.0×10^8	0	-	1.0×10^8	1	C	1.0×10^8	2	C	1.0×10^8	0	-	1.0×10^8
10^4	0	-	1.0×10^8	0	-	1.0×10^8	0	-	1.0×10^8	1	C	1.0×10^8	0	-	1.0×10^8	0	-	1.0×10^8	0	-	1.0×10^8

All BHs merge

First Objects

Bondi-Hoyle-Lyttleton Accretion

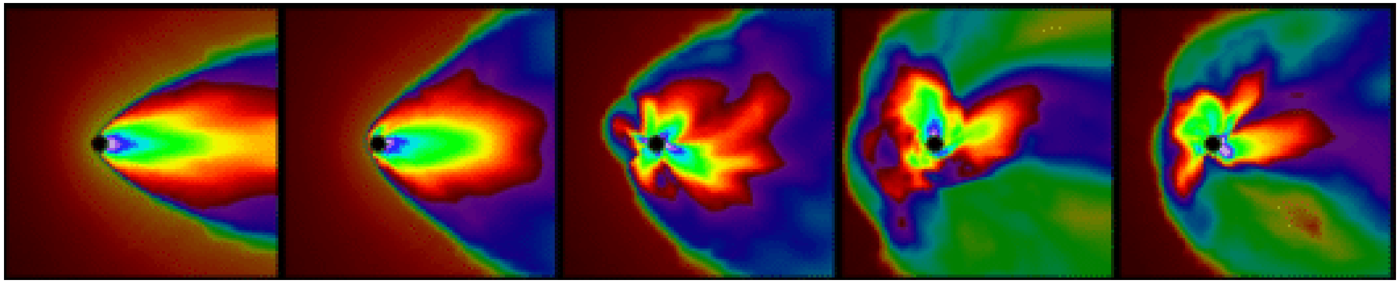

http://wwwmpa.mpa-garching.mpg.de/~mor/bhla.html

$$\dot{M}_{BHL} = 4\pi\rho \frac{G^2M^2}{(v^2 + c_s^2)^{3/2}} \qquad \therefore\ M = \frac{1}{M_0^{-1} - \alpha t}$$

$$t_\infty = 1.7 \times 10^6\,\mathrm{yr} \left(\frac{v}{100\ \mathrm{km\ s^{-1}}}\right)^{3} \left(\frac{n}{10^7\mathrm{cm^{-3}}}\right)^{-1} \left(\frac{M_0}{10^4 M_\odot}\right)^{-1}$$

$$\dot{M}_{BHL} = 0.6 M_\odot\,\mathrm{yr}^{-1} \left(\frac{v}{100\ \mathrm{km\ s^{-1}}}\right)^{-3} \left(\frac{n}{10^7\mathrm{cm^{-3}}}\right) \left(\frac{M_0}{10^4 M_\odot}\right)^{2}$$

$$\mathrm{cf} \qquad \dot{M}_E = 2 \times 10^{-4} M_\odot\,\mathrm{yr}^{-1} \left(\frac{M_0}{10^4 M_\odot}\right)$$

Accretion vs Merger

Tagawa, Umemura, Gouda, 2015, to be submitted

Critical mass accretion rate (below which the merger precedes)

$$\dot{M}_{\rm crit} / \dot{M}_{\rm BHL} = 0.34 \left(\frac{n_{\rm gas}}{10^{7}\,{\rm cm}^{-3}} \right)^{-1} \left(\frac{\rho_{\rm BH}}{10^{7} M_{\odot}\,{\rm pc}^{-3}} \right)^{0.8} \approx 10^{3-4} \dot{M}_{\rm E}$$

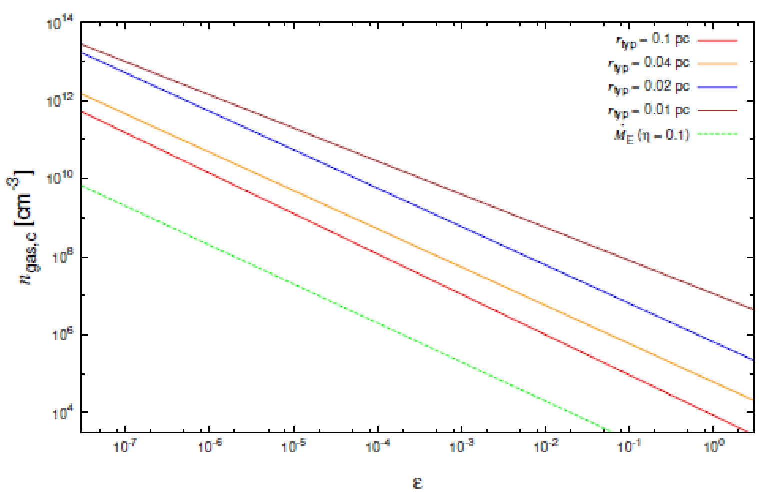

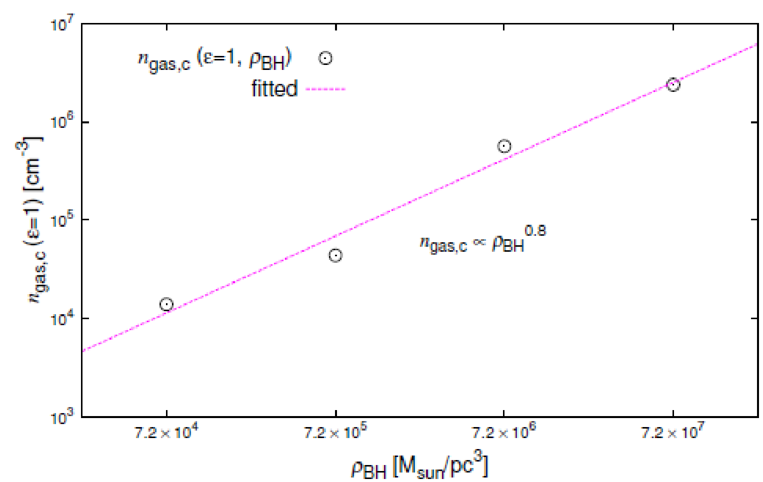

Figure 6. The plots represent the critical gas number density as a function of the BH density. The line is the curve fitted by $\left(\frac{n_{\rm gas,c}}{1\ {\rm cm}^{-3}}\right) = a \left(\frac{\rho_{\rm BH}}{1.0\ M_{\odot}/{\rm pc}^3}\right)^b$.

Direct Collapse to Supermassive Stars with $10^{4\text{-}6} M_{\odot}$

- **Compton drag by CMB radiation**
  Umemura, Loeb, Turner 1993

- **Supression of H2 Cooling**
  Bromm & Loeb 2003
  Begelman, Volonteri & Rees 2006
  Inayoshi & Omukai 2012

- **Heating by DM annihilation**
  Spolyar, Freese, Gondolo 2008

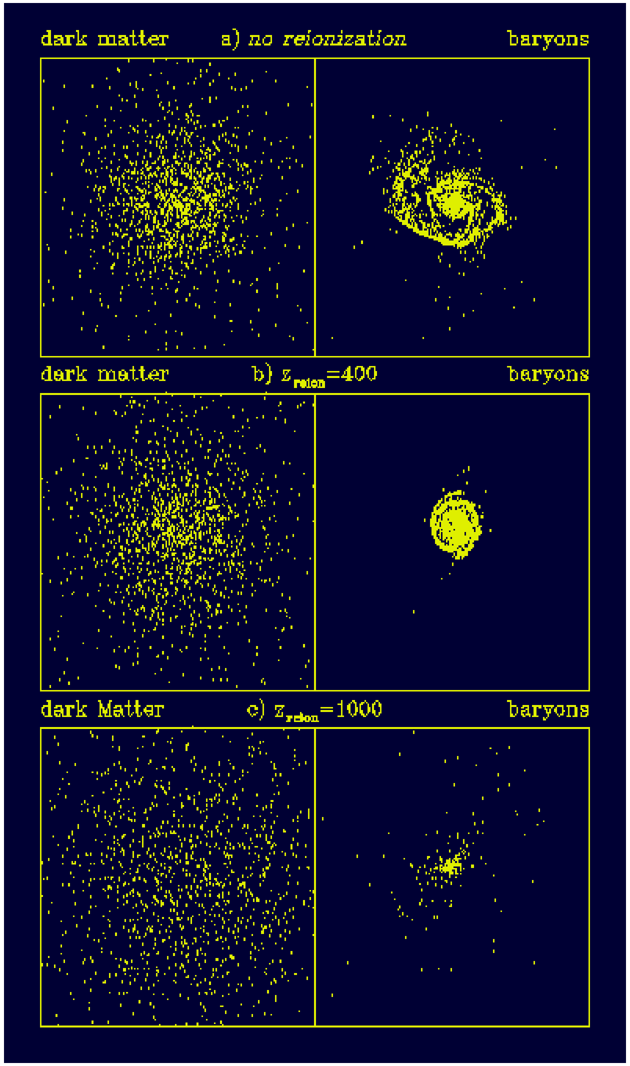

General Relativistic Instability

Baumgarte & Shapiro 1999, ApJ, 526, 941

Rapidly rotating supermassive star
in equilibrium

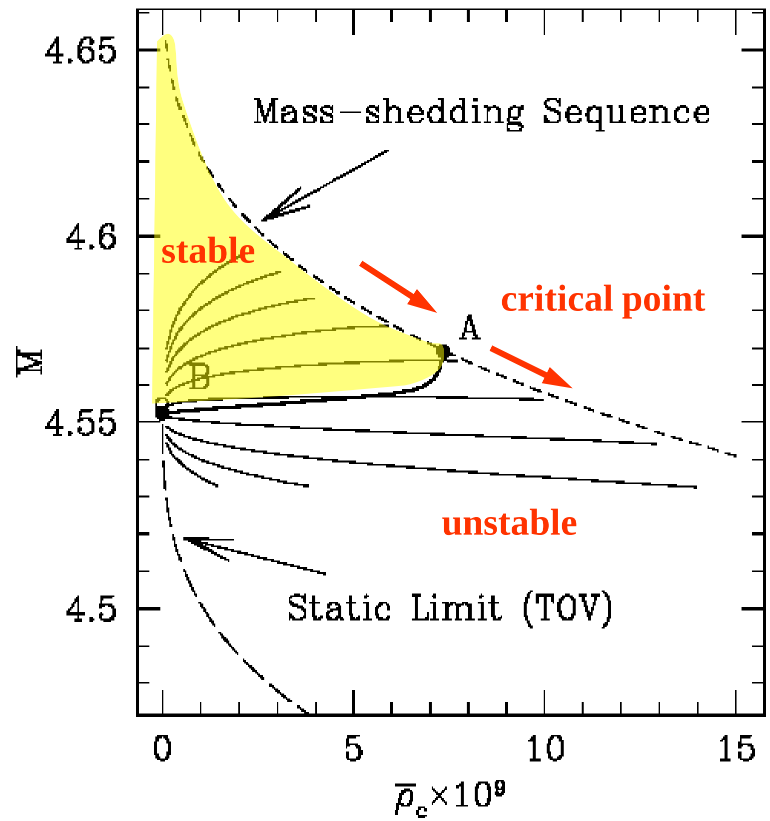

Post-Newtonian

Saijyo, Baumgarte, Shapiro & Shibata
(2002, ApJ, 569, 349)

Rigid rotating SMS Þ collapse

Numerical Relativity

Shibata & Shapiro 2002, ApJ, 572, L39

g=4/3 Polytrope (radiation-dominated)

Kerr BH with *a* » 0.75

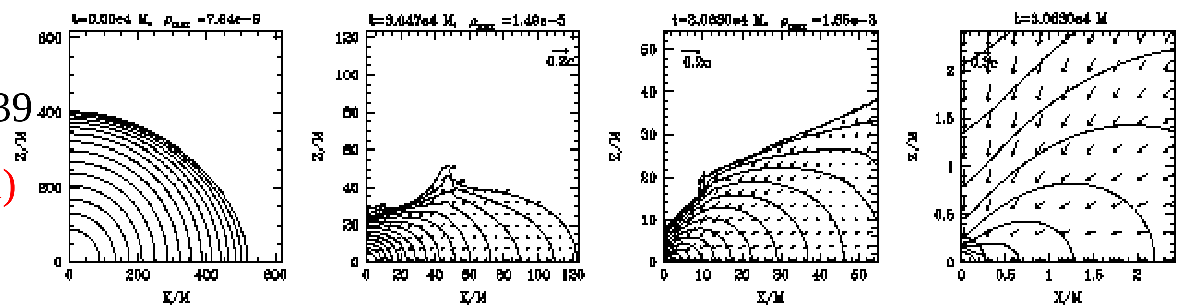

But, no **General Relativistic Radiation Hydrodynamic (GR-RHD)** simulations !

Difficulties in GR-RHD

A) In relativistic motion, the steady state of radiation fields cannot be assumed.

[Time-dependent transfer equation should be solved.]

C) Light bending, frame-dragging, and gravitational redshifts should be included.

[Transfer should be solved along the geodesics.]

B) Causality should be retained.

[We should solve the propagation of wave fronts in proper time.]

D) GR energy-momentum tensor of radiation should be obtained.

[LNRF (locally non-rotating reference frame) should be transformed to the curved space.]

We have overcome all these difficulties !

Vermeer

Master of light

Variable Eddington-tensor Radation-hydrodynamics with Metric Enchained Ray-tracing

General Relativistic Radiation Transfer
Radiation Hydrodynamics in Curved Space

Rhota Takahashi & Masayuki Umemura

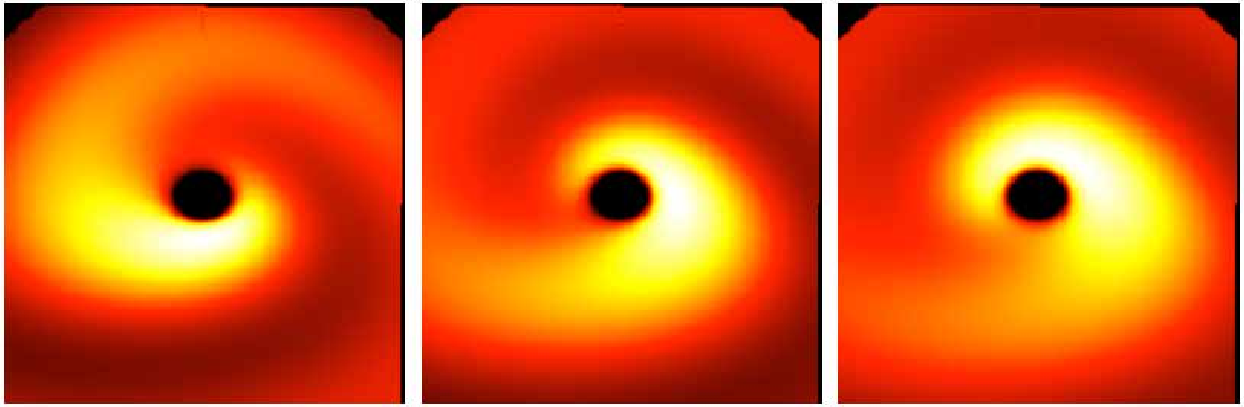

GR Radiation Transfer

General Relativistic Boltzmann Equation of Photons

$$\frac{d\mathcal{I}_\nu}{d\lambda} = \mathcal{E}_\nu - \mathcal{A}_\nu \mathcal{I}_\nu$$

$\mathcal{I}_\nu \equiv \dfrac{I_\nu}{\nu^3}$: Invariant specific intensity

$\mathcal{E}_\nu \equiv \dfrac{\eta_\nu}{\nu^2}$: Invariant emissivity

$\mathcal{A}_\nu \equiv \nu\chi_\nu$: Invariant extinction

- **Solve GR radiative transfer along geodesics**
- **Obtain invariant specific intensity in 6D phase space**

Dynamical Test 2: Photon wave front from a rotating hot spot

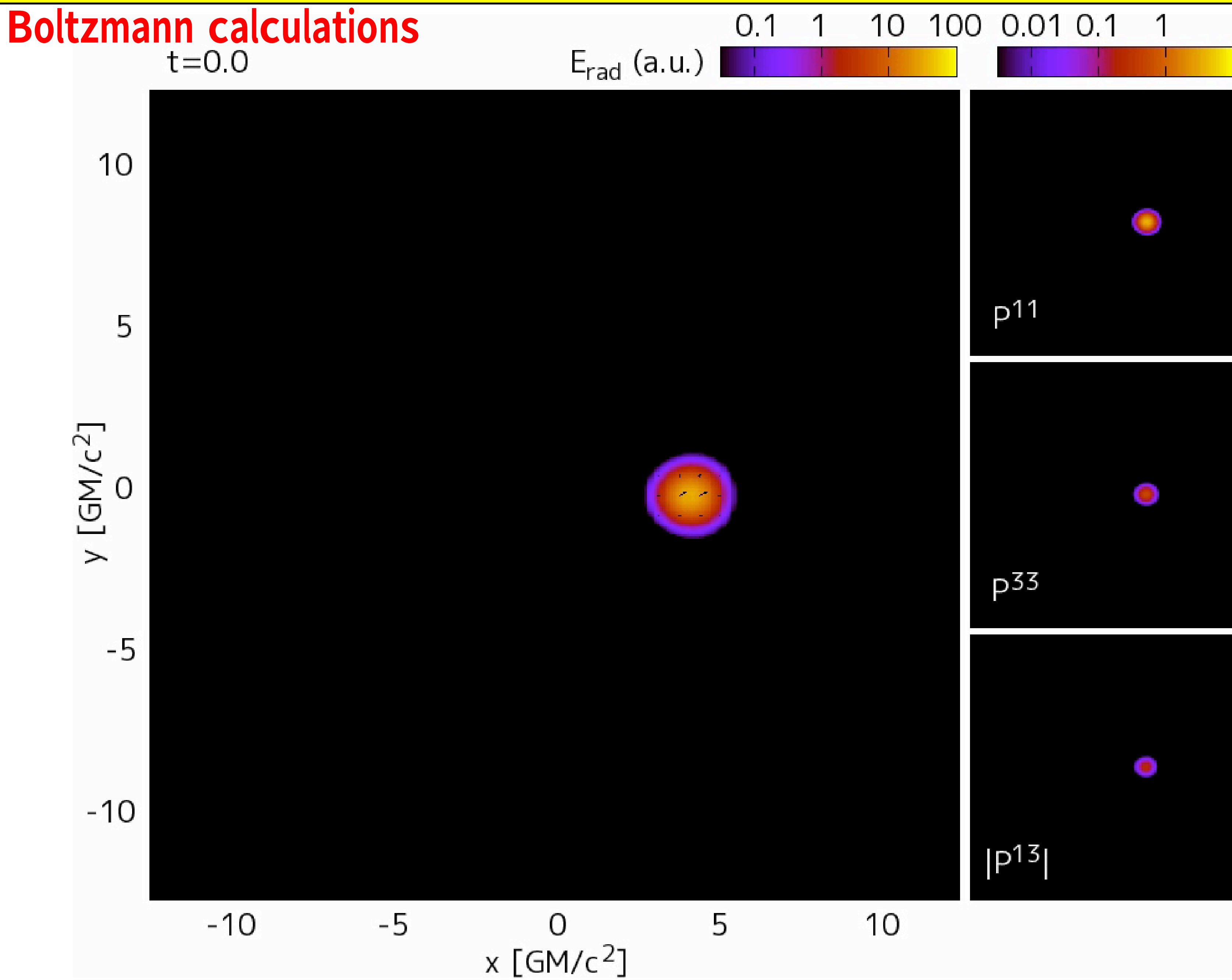

Boltzmann calculations

Ray-tracing calculations

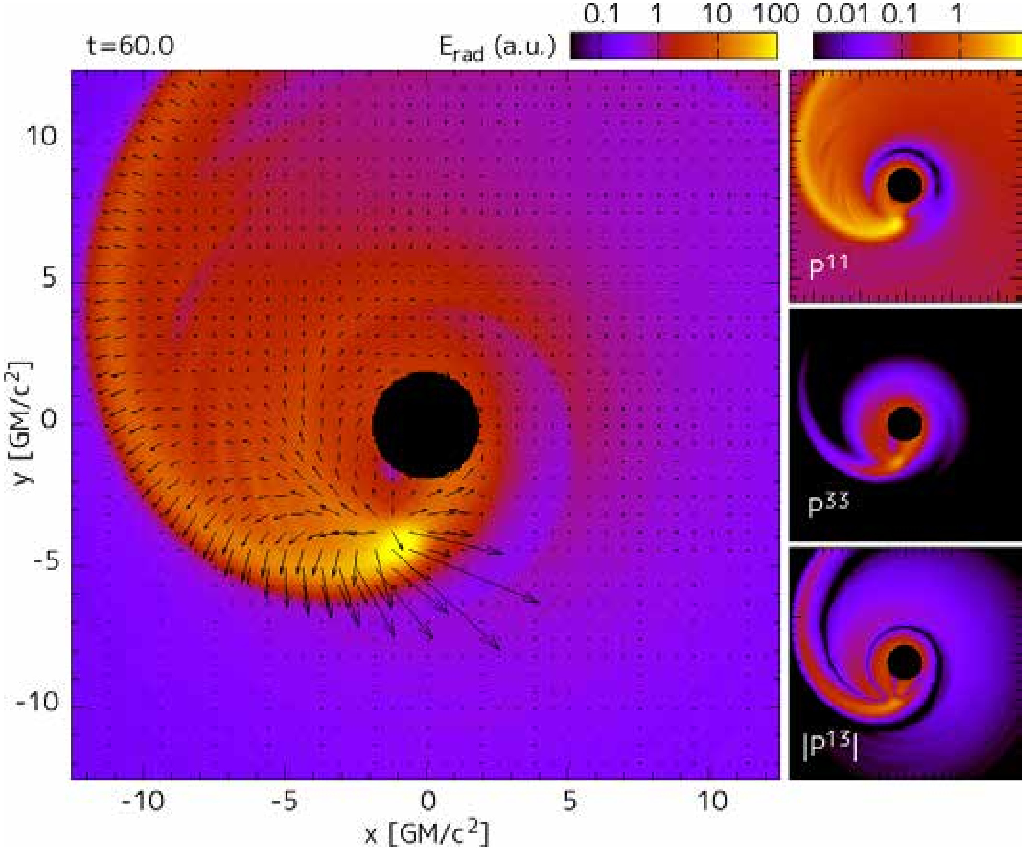

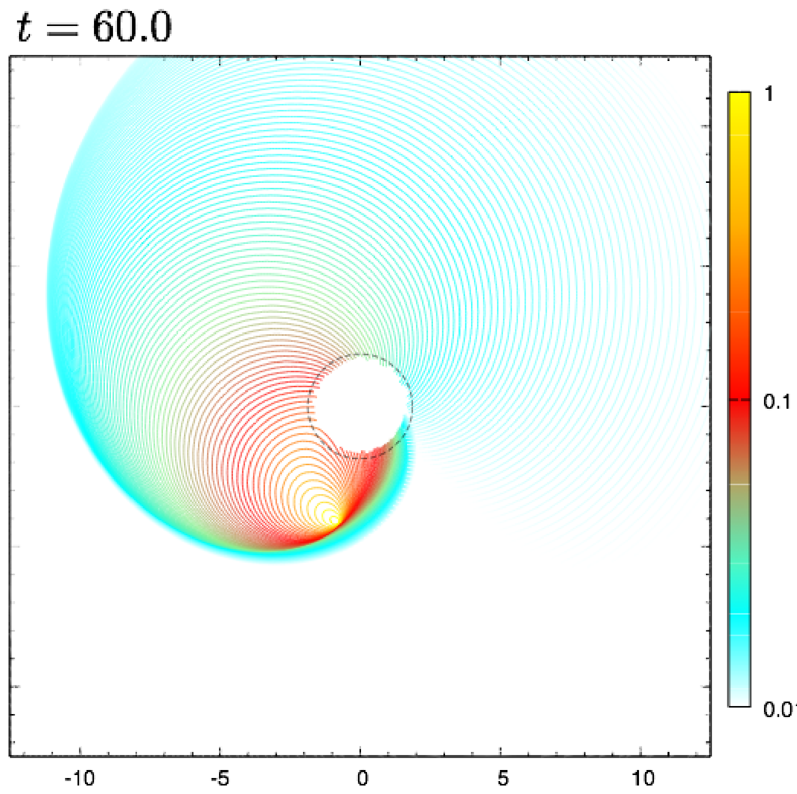

N_i (r)=90, N_j (f) =256

Geodesics=4608

Primordial BHs in Inflation

Carr & Lidsey, Phys. Rev. D 48, 543 (1993)

Yokoyama, A&A, 318, 673 (1997); Phys. Rep., 307, 133 (1998)

Kawasaki, Sugiyama, Yanagida, Phys. Rev. D 57, 6050 (1998)

Bringmann, Kiefer, & Polarski, Phys. Rev. D 65, 024008 (2002)

Kawaguchi et al. MNRAS, 388, 1426 (2008)

Drees & Erfani, JCAP, 4, 5 (2011); JCAP, 1, 35 (2012)

Kohri, Lin & Matsuda, Phys. Rev. D 87, 103527 (2013)

Erfani, Phys. Rev. D 89, 083511 (2014)

Clesse & Garcia-Bellido, Phys. Rev. D 92, 023524 (2015)

Massive Primordial BHs from Hybrid Inflation

Clesse & Garcia-Bellido, Phys. Rev. D 92, 023524 (2015)

PBHs produced from the collapse of large curvature perturbations generated during a mild-waterfall phase of hybrid inflation

Dark matter candidates
Swiss-cheese-like structure of the Universe (leading to apparent accelerated cosmic expansion)

1. Lifetime of primordial black holes
2. Light element abundances
3. Extragalactic photon background
4. Galactic background radiation
5. Femtolensing of gamma-ray bursts
6. Capture of PBHs by neutron stars
7. Microlensing surveys
8. CMB spectral distortions

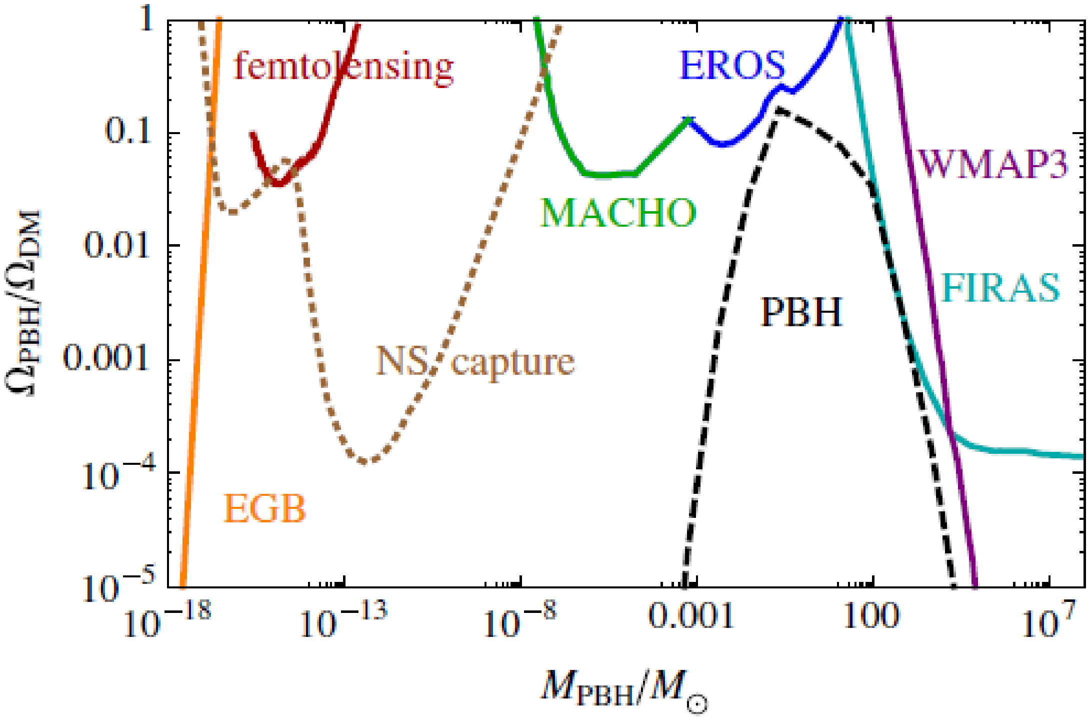

Constraint from Cosmic Reionization Epoch

Planck 2015 results $z_{\rm reion} = 8.8^{+1.7}_{-1.4}$

Minimum photon number rate (Madau, Haardt, Rees 1999):

$$\dot{n}_{\rm rec} = \frac{n(z=0)}{t_{\rm rec}} = 4.1\times 10^{-23}\left(\frac{1+z}{10}\right)^3\left(\frac{\Omega_b h_{70}^2}{0.04}\right)^2 C_5\ \mathrm{s^{-1}\ cm^{-3}}\ \text{<comoving>}$$

Ionizing photon number rate from accreting BHs

Eddington luminosity density:

$$L_E = \frac{4\pi G c m_p}{\sigma_T}\Omega_{BH}\rho_c = 2.4\times 10^{-26}\,\Omega_{BH}\left(\frac{\Omega_b h_{70}^2}{0.04}\right)\ \mathrm{erg\ s^{-1}\ cm^{-3}}$$

$$\dot{n}_\gamma \approx \frac{L_E}{h\nu_L} f_{UV}\cdot f_{esc}$$

$$= 5.3\times 10^{-22}\left(\frac{\Omega_{BH}}{10^{-4}}\right)\left(\frac{f_{UV}}{0.1}\right)\left(\frac{f_{esc}}{0.1}\right)\left(\frac{\Omega_b h_{70}^2}{0.04}\right)\ \mathrm{s^{-1}\ cm^{-3}}\ \text{<comoving>}$$

Constraint from Planck 2015

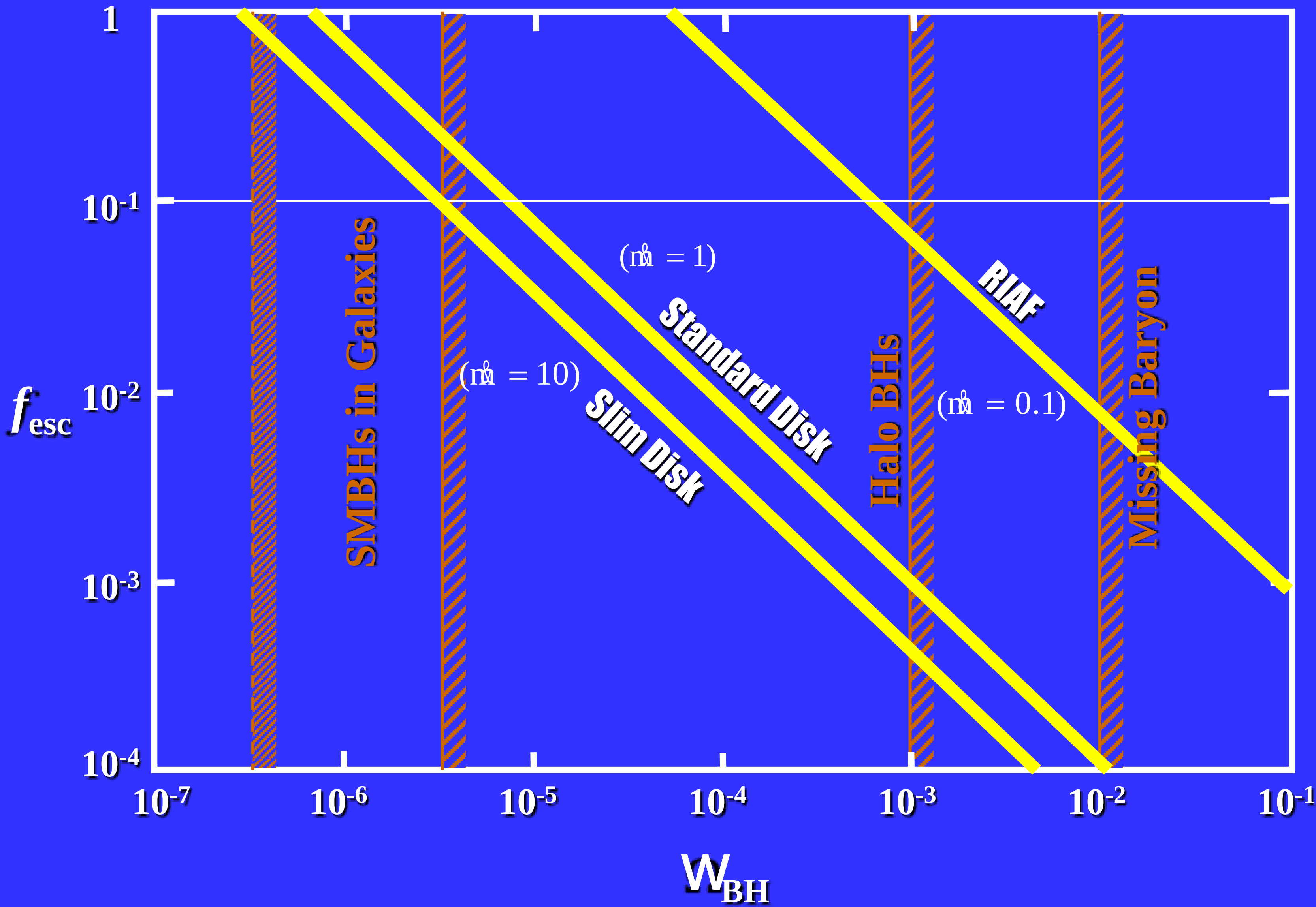

Conclusions

Ø **Formation of SMBHs is one of greatest mysteries in astrophysics.**

Ø **All BHs in the first objects can merge in 10^7 yr.**

Ø **BH Merger is faster than accretion, if mass accretion rate is less than 10% of the Bondi-Hoyle-Lyttleton accretion rate.**

Ø **GR-RHD simulations on SMS are coming soon (in two years?)**

Ø **Formation of PBHs is a peace of the puzzle.**

Ø **Constraint on PBHs from cosmic reionization (Planck 2015) is**

$$10^{-4} < f_{esc}\, W_{BH} < 10^{-7}$$

Thank you for your attention